Free Space Communication Enabled by Directly Modulated Quantum Cascade Laser

Xiaodan Pang[1,4,8], Richard Schatz[1], Mahdieh Joharifar[1], Hamza Dely[2], Laureline Durupt[3], Gregory Maisons[3], Djamal Gacemi[2], Rafael Puerta[5,1], Thomas Bonazzi[2], Lu Zhang[6], Sandis Spolitis[4], Yan-Ting Sun[1], Vjačeslavs Bobrovs[4], Xianbin Yu[6,7], Angela Vasanelli[2], Carlo Sirtori[2], Oskars Ozolins[4,8,1]

[1]*Department of Applied Physics, KTH Royal Institute of Technology, 106 91 Stockholm, Sweden.* xiaodan@kth.se
[2]*Laboratoire de Physique de l'ENS, Département de Physique, École Normale Supérieure, Université PSL, Sorbonne Université, Université Paris Cité, CNRS, 75005 Paris, France.*
[3]*mirSense, 1 rue Jean Rostand, 91400 Orsay, France.*
[4]*Institute of Telecommunications, Riga Technical University, 1048 Riga, Latvia.* oskars.ozolins@rtu.lv
[5]*Ericsson Research, Ericsson AB, 164 83 Stockholm, Sweden*
[6]*College of Information Science and Electrical Engineering, Zhejiang University, Hangzhou 310027, China.*
[7]*Zhejiang Lab, Hangzhou, China.*
[8]*RISE Research Institutes of Sweden, 164 40 Kista, Sweden.*

Abstract: We summarize our recent experimental studies of free-space communications enabled by directly modulated quantum cascade lasers at both MWIR and LWIR regions. Different detector types with different characteristics are compared. © 2024 The Author(s)

1. Introduction

The mid-infrared (MIR) region contains two atmospheric transmission windows, namely, the mid-wave infrared (MWIR, 3-5 µm) and the long-wave IR (LWIR, 8-12 µm). Compared with the near-IR telecom band around 1.5 µm, they possess unique merits for future free-space optical (FSO) communications: they experience lower Mie scattering from particles in the atmosphere, and their longer wavelengths ensure higher resilience against turbulence-induced scintillation effect [1]. Moreover, they have more relaxed eye-safety threshold [2]. Therefore, these key limitations of FSO systems can be effectively addressed for practical applications. To date, there are mainly three categories of methods to realize MIR FSO transmissions: the wavelength-conversion approach [3]-[5], external modulation [6]-[8], and directly modulated laser sources [9]-[14]. The wavelength-conversion approach benefits from the reuse of fiber-optic components and existing multi-dimensional multiplexing schemes to achieve high overall system data rate [4]. On the other hand, lower energy consumption, smaller footprint, and higher integrability can be better achieved with MIR semiconductor optoelectronic sources, modulators, and detectors. The recent technological breakthroughs in unipolar quantum optoelectronics, including high-bandwidth quantum cascade laser (QCL), quantum cascade detectors (QCD) and Stark-effect MIR modulators, provide a promising pathway for MIR FSO transceivers. Figure 1 presents a non-exhaustive summary of recent demonstrations in both MWIR and LWIR with >10 Mbps transmission rate with these three approaches. The evolution of demonstrated single-channel data rate with respect to the reporting year is shown in Fig. 1 (a). One can observe that significant progress following all three technological roadmaps has been made during the past decade. Considering utilizing multi-dimensional multiplexing schemes, the wavelength-conversion approach has

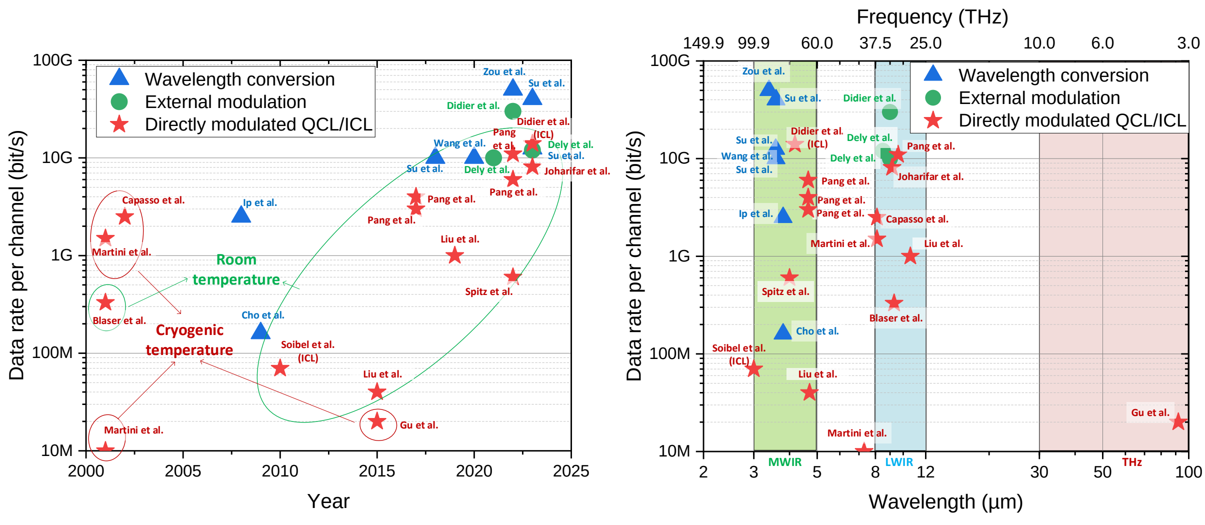

(a) **(b)**

Fig. 1. Summary of mid-IR FSO demonstrations with different schemes, showing (a) the year of publication for each work and (b) the corresponding wavelength / carrier frequency used in each study. Note: This summary is non-exhaustive.

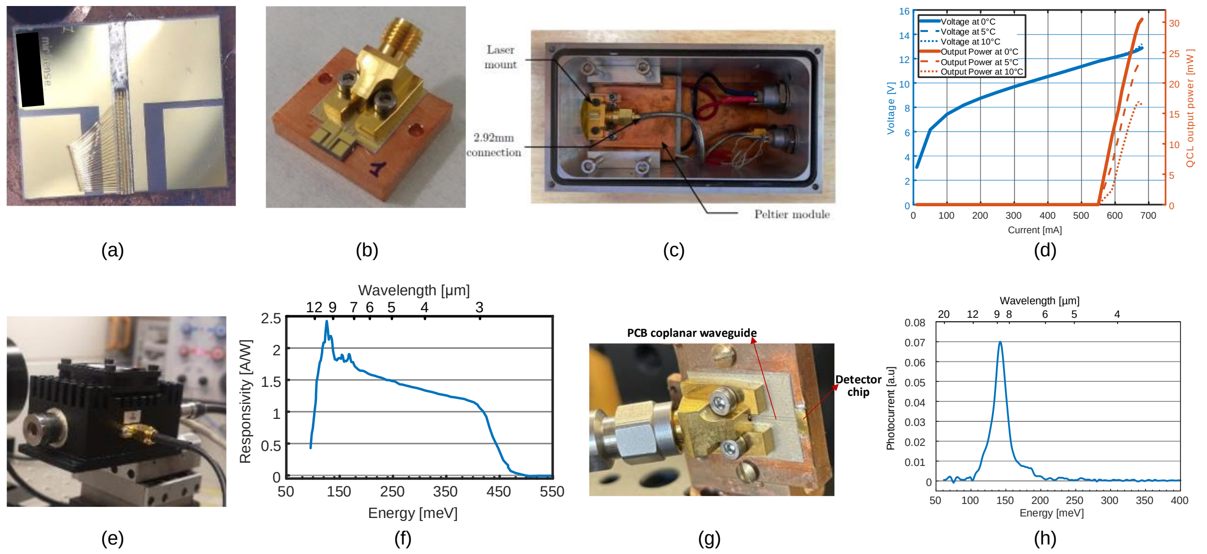

Fig. 2. Optoelectronic components for mid-IR FSO demonstrations. (a) Picture of a typical QCL submount. (b) QCL module after RF bounding of the submount. (c) Peltier mount hosting the QCL module. (d) Typical QCL L-I-V curves with respect to operational temperature. (e) A commercial MCT detector used for FSO demonstration. (f). The MCT responsivity spectrum. (g) A typical appearance of RF bounded QCD/QWIP. (h). Responsivity spectrum of the employed QCD.

achieved overall system data rate of >100 Gbps [3]-[5]. Notably, room-temperature LWIR FSO based on both external modulator and directly modulated lasers have achieved over 10 Gbps per-channel rate, all happened during the past two years. Figure 1 (b) shows the demonstrated single-channel data rate with respect to the spectral band. One can see that all the wavelength-conversion works focused on the MWIR band to ensure conversion efficiency. Moreover, the interband cascade lasers (ICL) also show promising results in the MWIR region. The LWIR band, in contrast, is dominated with the external modulation and the directly modulated QCL (DM-QCL) approaches. THz-QCL also appears in the landscape, which, however, can still only support Mbps scale data rate with cryogenic operation.

In this report, we focus on our recent effort in employing DM-QCL for FSO transmissions in both the MWIR and the LWIR bands. We show the potential of such a scheme in supporting high data rate with different types of detectors, including commercial HgCdTe (mercury cadmium telluride, MCT) detector, QCD and quantum-well IR detector (QWIP). The operational conditions and system characteristics are evaluated and discussed.

2. Unipolar quantum optoelectronic components

At the FSO transmitter we use QCL chips fabricated by mirSense, both operating in MWIR and LWIR. Figure 2 (a) depicts a typical QCL submount picture hosting the QCL laser chip. The QCLs are designed to operate in continuous wave (CW) mode with a few tens of milliwatt output power. The RF bounded QCL module is shown in Fig. 2 (b), where a 2.92-mm RF coaxial interface is connected to the QCL submount through a coplanar waveguide on a printed circuit board (PCB). The QCL module is then placed in a Peltier mounting module for temperature control during operation, as shown in Fig. 2 (c). Figure 2 (d) depicts typical QCL L-I-V curves with respect to different operational temperature points, and one can see that lower temperature yields higher output power due to faster heat dissipation.

At the receiving end, we used different types of detectors, namely, a commercial MCT photovoltaic detector, QCD, and QWIP. Figure 2(e) shows a picture of the MCT detector module used in both MWIR and LWIR FSO experiments. Its response spectrum, as shown in Fig. 2(f), indicates a broad operational range covering both transmission windows, which can potentially support wavelength-division multiplexing (WDM) configurations with a single detector design. However, the drawback of such MCT detectors is that their bandwidth is often limited to the sub-GHz scale, resulting in a bottleneck in the system's end-to-end frequency response. Alternatively, we have employed higher-bandwidth QCD and QWIP detectors to overcome such limitations. However, the detector responsivity and noise performance of these broadband components are comparatively lower than that of the MCT, imposing higher requirements on the received signal power and SNR. This translates to a demand for higher emitting power from the QCL and stricter beam alignment and focusing accuracy. These trade-offs are reflected in the highest achievable data rates in FSO systems with different laser-detector configurations during experimental demonstrations. Figure 2(g) shows a picture of a QCD module used in our demonstrations, which also resembles the appearance of the QWIP module. Another aspect of both QCD and QWIP is their relatively narrower responsivity spectrum compared to the MCT. As shown in Fig. 2(h), the responsivity spectrum of a LWIR QCD is locally confined around 9 μm. Therefore, specific detectors operating at different wavelengths should be designed for WDM.

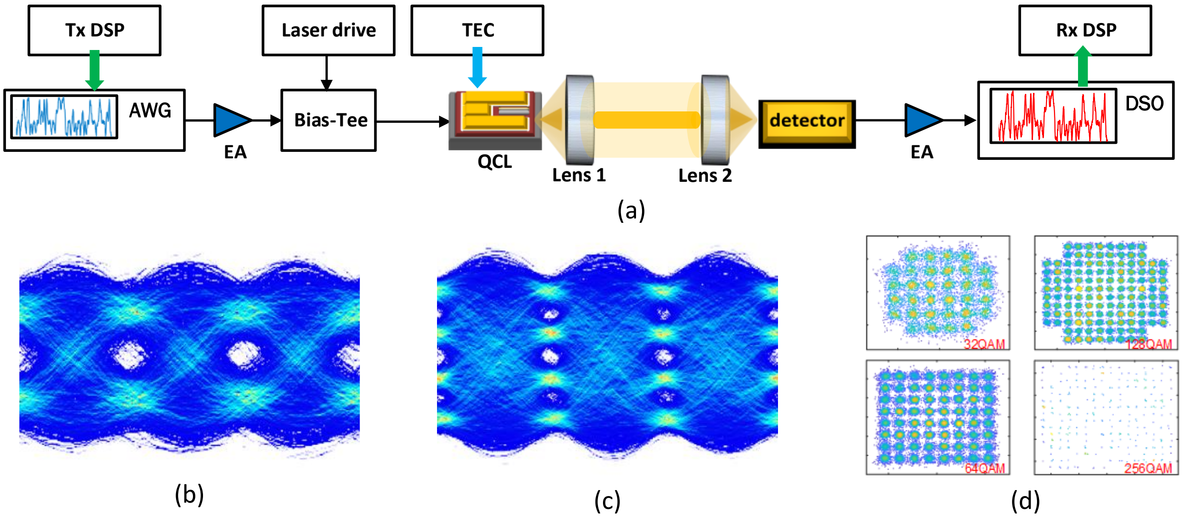

Fig. 3. Experimental demonstrations of mid-IR FSO enabled by DM-QCL. (a) A typical experimental setup. (b) Selected eye diagram of NRZ after FSO transmission. (c) Selected eye diagram of PAM4 after FSO transmission. (d) Selected constellation diagrams for DMT transmission.

3. Experimental demonstrations

We have performed a series of experimental demonstrations with DM-QCL in both the MWIR and the LWIR bands. Figure 3 (a) shows a representative experimental setup. Signals of different modulation formats are generated with an arbitrary waveform generator (AWG) after transmitter digital signal processing (DSP) routine. The signal is modulated to the bias current of the DM-QCL, which is normally temperature controlled. The emitted beam from the QCL is collimated and collected with a pair of lenses. The received signal is focused on the detector to generate electrical output, which is amplified and sampled with a real-time digital sampling oscilloscope (DSO) for offline DSP processing and signal demodulation. In the MWIR, we first demonstrated a 3-Gbps close-proximity FSO coupling with NRZ, PAM4 and PAM8 with a room-temperature 4.65-µm DM-QCL and the commercial MCT detector. Then we improved on the spectral efficiency and achieved 4-Gbps using the same laser and detector with both PAM4 and DMT signaling. With a continuous effort in improving the beam collimation and receiver coupling, we further improved the received signal SNR and increased the system data rate to 6 Gbps. In the LWIR region, we have tested different types of detectors, including the same MCT detector that was used for MWIR transmissions, an upgraded MCT detector with enhanced bandwidth, a passive QCD, and metamaterial-patterned detectors. Different modulation formats, including multilevel PAM signals and DMT signals were also tested and compared. Up to 5.1 Gbps DMT and up to 8.1 Gbps PAM8 transmissions are achieved with a 9.15- µm DM-QCL and the same MCT detector used for MWIR. We recently also reported up to 11 Gbps transmission with the configuration of a 9.6-µm DM-QCL and the fully passive QCD. Figure 3 (b)-(d) illustrates example eye diagrams and constellation diagrams of NRZ, PAM4 and DMT after LWIR FSO transmissions. Higher data dates with other laser-detector configurations are yet to be reported.

4. Conclusion

We summarize our recent research effort in pushing forward the MIR FSO with focus on using DM-QCL-based transmitter. By extrapolating the increase in achievable data rate, we expect to close the gap between the MIR FSO and fiber-optic communication systems soon. Further efforts include developing hardware and schemes for coherent modulation and reception of MIR FSO signals and exploring potential multi-dimensional multiplexing.

5. Acknowledgement

This work was supported in part by the EU H2020 cFLOW Project (828893), in part by the Swedish Research Council (VR) project 2019 05197 and project 'BRAIN' 2022 04798, in part by the COST Action CA19111 NEWFOCUS, in part by the LZP FLPP project 'MIR FAST' lzp-2023-1-0503, and in part by the strategic innovation program Smarter Electronic Systems - a joint venture by Vinnova, Formas and the Swedish Energy Agency A-FRONTAHUL project (2023-00659).

6. References

[1] E. Leitgeb *et al.*, *Proc. ICTON* 2010, p. Th.B3.1.
[2] A. Delga *et al.*, *Quantum Sensing and Nano Electronics and Photonics XVI* 2019, p. 1092617.
[3] Y. Su *et al.*, Optics Express **31**, 15156-15169 (2023).
[4] K. Zou *et al.*, Nat Commun. **13**, 7662 (2022).
[5] A. E. Willner *et al.*, Opt. Commun. **541**, 129518 (2023).
[6] H. Dely *et al.*, Laser & Photonics Reviews **16** (2021).
[7] H. Dely *et al.*, Optics Express **31** (2023).
[8] P. Didier *et al.*, Advanced Photonics **4**, 056004 (2022).
[9] O. Spitz *et al.*, IEEE J. Quantum Electron. **28**, 1-9 (2022).
[10] P. Didier *et al.*, Photonics Research **11** (2023).
[11] X. Pang *et al.*, Phys. Status Solidi A **218**, 2000407 (2021).
[12] X. Pang *et al.*, J. Lightwave Technol. **40**, 2370-2377 (2022).
[13] M. Joharifar *et al.*, *Proc. OFC 2023*, p. Th1H.1.
[14] X. Pang *et al.*, *Proc. OFC 2022*, p. Th4B.5.